



## Statistical Features of the Aftershock Sequence after the Mw8.3 Strong Earthquake Near Illapel, Chile in 2015

K. Yanev<sup>1</sup>, D. Gospodinov<sup>1</sup>, B. Ranguelov<sup>2</sup>

<sup>1</sup>Faculty of Physics, Plovdiv University "Paisii Hilendarski", Tsar Asen str, 24, Plovdiv, Bulgaria

<sup>2</sup>Faculty of Geoexploration, University of Mining and Geology "St. Ivan Rilski", Sofia, Bulgaria

**Abstract.** A strong earthquakes occurred in Chile on the 16<sup>th</sup> of September, 2015 with a magnitude of Mw=8.3, near the Kokimbo region. The main quake had a duration of 3 minutes and was followed by several aftershocks within the next 30 minutes, some with a magnitude greater than Mw>6. In this study we compiled aftershock catalog data, lasting 8 months after the main shock. The initial statistical analysis of the catalog, completed with the ZMAP6.5 software, showed a relatively low b-value, which meant that there was a high number of weaker aftershocks in the series. After identifying the completeness magnitude of  $M_0=3.5$ , only events with a magnitude equal to or higher than the magnitude of completeness were analyzed. The RETAS model was used in terms of finding a relevant time model, describing the drop in aftershock activity during the period. The estimated best-fit model offers the opportunity of describing the aftershock rate evolution in time for the studied region. The model confirms such a pattern of aftershock clustering, in which aftershocks group up in time, not only along strong events, but can also form clusters after weaker shocks.

**Keywords:** stochastic modeling, RETAS model, aftershocks

### 1. INTRODUCTION

The relative movement between the tectonic plates along their boundaries is the main reason for Earth's seismicity. There are three types of boundaries between the plates: divergent, convergent and transform boundaries. Divergent types of boundaries occur where two given plates slide apart from each other thus forming a gap. Convergent boundaries are the other way around. They occur when two given plates slide toward each other making a collision and thus forming mountain chains for example. Transform boundaries occur when two given plates grind past each other along transform faults and plates are neither created nor destroyed.

With the ongoing subduction process, some of the ocean's floor sediments along with pieces of the ocean's crust fall into the so called process of obduction. During this process the sediments and the ocean crust are being shifted in along the South-American plate faults. As a result, the leading edge of the South-American plate deforms, thus increasing its vertical thickness

instead of sideways extension at the point of impact. This is the reason for the Formation of the Andes, one of the longest mountain chains on Earth with length of 7,000km and average height of 4,000m. Many of the mountain peaks are active volcanoes due to this process

In terms of judging the seismic hazard, time distribution of earthquakes is vital. While the Poisson process is the main model for describing time distribution for strong earthquakes, for the aftershocks has to be used a statistical model which has to read through the event's clustering.

While strong earthquakes are spaced along the boundaries of the tectonic plates, the aftershocks of a given earthquake cover the area around the fault on which the main event happened. On Fig. 1 are given the epicenters of aftershocks after the strong earthquake with magnitude of  $M=9.1$  near Sumatra in December 2004. On the left side, the green triangle illustrates the epicenter of the main event, while the red dots are the epicenters of all aftershocks with a magnitude greater than  $M>4.0$ . On the

rights side is illustrated the spatial distribution of aftershocks in time in a profile which passes longitudinally along the fault. These epicenters show that the spatial distribution of aftershocks typically characterizes with a hierarchical structure as some aftershocks can trigger their own spatial aftershock clusters

On September 16th, 2015 a strong earthquake struck in the north Chilean region Coquimbo with a magnitude of  $M=8.3$ . The town of Illapel takes the most amount of damage as the first

tsunami waves reach within minutes. The event was followed by numerous aftershocks. The sequence obviously is a complex one (see Gospodinov et al., 2007) and common statistical models are inappropriate to distinguish the temporal details. The purpose of the present paper is to examine some of the statistical features of the aftershock sequence that followed the 2015 Illapel earthquake and more specifically, the stochastic model of its temporal distribution.

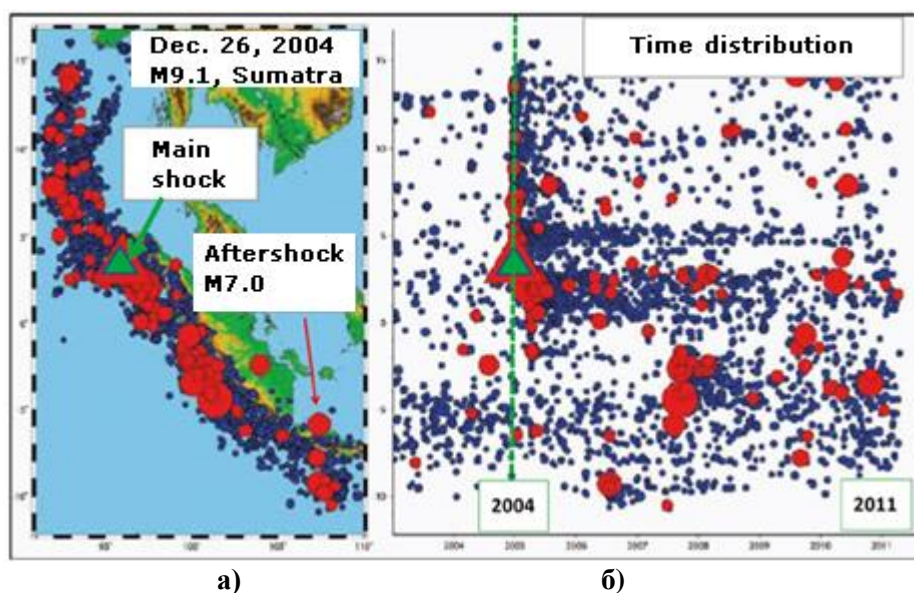


**Fig.1** Epicentral map of the aftershocks after the strong M9.1 earthquake near Sumatra in December, 2004: a) Epicenter card - the green triangle shows the epicenter of the strong main earthquake and the red circles are epicenters of the aftershocks with magnitudes  $M \geq 4.0$ ; b) Distribution of the aftershocks in time by profile, which runs longitudinally to the fault

## 2. GEOTECTONIC SETTINGS OF THE ILLAPEL EARTHQUAKE REGION

The M8.3 earthquake occurred near Illapel in 2015 is near the Kokimbo region. There the seismicity is generally generated by the relative movement of the Nazca plate relative to the South-American plate. The Nazca plate is one of the main tectonic plates which form the Earth's crust. It is located in the Pacific ocean near the west coast of South America. The current subduction process of the plate along the Peru-Chilean trench, also known as the Atakama trench, is responsible for the formation of the Andes mountain chain.

The Nazca plate is a relatively “young” plate in terms of age of its rock, as well as in terms of its existence as an independent tectonic plate. The subduction of the Nazca plate under the South-American plate along the Atakama trench (Fig.2) is tied to numerous earthquakes, some of which stand out with their strength and following tsunamis or landslides. The strongest earthquake registered on Earth, known as the Valdivia earthquake happens here with a magnitude of  $M=9.5$ . Again, in this region, on the 16th of September 2015 happens the Illapel earthquake with a magnitude of  $M_w=8.3$ , whose aftershock activity is still runs today and is the main interest of this article (Fig.3).



**Fig.2** The process of subduction of the Nazca plate under the South American plate ([https://en.wikipedia.org/wiki/2015\\_Illapel\\_earthquake](https://en.wikipedia.org/wiki/2015_Illapel_earthquake))

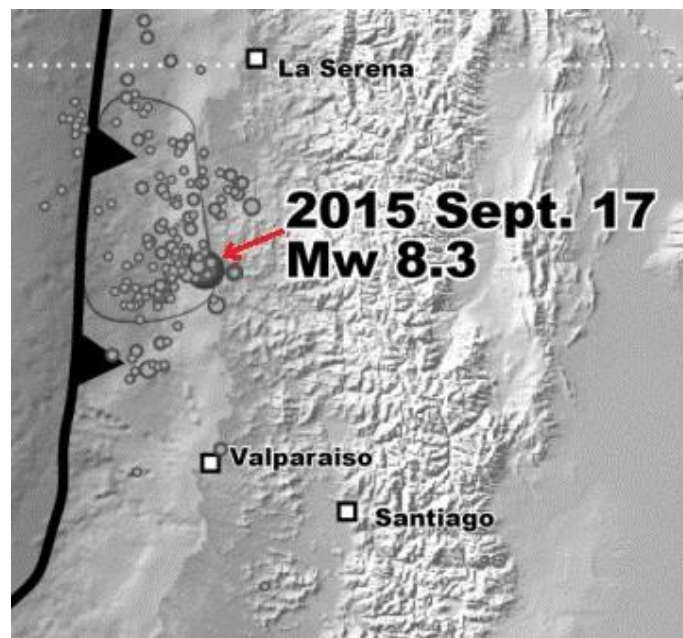


**Fig.3** Mainshock and aftershock epicenters of the 2015 Illapel sequence

The Nazca plate has both divergent and convergent boundaries from west to east respectively and contains three big mid-ocean ridges. To the east it goes under the South-American plate with the greatest subduction velocity of  $61\pm 3$  mm/year. To the west it stretches again with the greatest velocity of  $120\pm 3$  mm/year. To the north and south occur

divergent boundaries between the Cocos and Antarctic plate respectively (Fig.1).

### 3. AFTERSHOCK DATA AND STATISTICAL ANALYSIS

#### 3.1 Historical seismicity of the region

On May 22nd, 1960 the Great Chilean earthquake struck, also known as the Valdivia

earthquake. It had a magnitude of  $M=9.5$  and duration of over 10 minutes, which makes it the strongest registered earthquake on Earth. The town of Valdivia is the most affected from the entire region with huge destruction. The quake forms tsunami waves with height of 25m., who struck the Chilean coastline. The main tsunami dashes through the Pacific ocean reaching the town of Hilo, Hawaii and destroying it completely. At Japan and the Philippines, waves with height greater than 10m. were registered, 10,000km away. This was a megathrust earthquake, happened as a result of sudden release of energy between the Nazca and South-American plate along the Atakama trench. The subduction zones are well known for their ability to create strong earthquakes like this, as their structure proposes the accumulation of huge tension and energy before being violently released.

### 3.2 Aftershock Data

For the Illapel earthquake of 2015, the catalog data for the aftershock series was compelled.

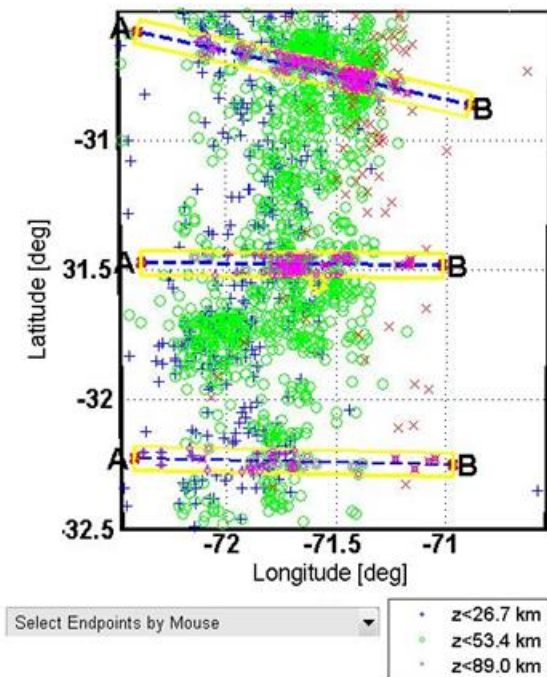


**Fig.4** Epicenter map of the aftershocks in the study sequence. The dashed lines show three profiles along which the epicentral depth increases, confirming the subduction process

We used the international center for seismologic information to the United States Geological Survey to do the job. 1752 events were identified in an area between these geographic vertices:

- 70.7W, -30.5S - 72.7W, -30.5S
- 72.7W, -32.5S - 70.7W, -32.5S

The initial statistical analysis is completed using the ZMAP6.5 software (Wiemer, 2001). Fig 5.1 shows the results of the data analysis as the goal was to define the parameters of the Gutenberg-Richter law for the research data. The relatively low  $b$  value shows that the series has an increased number of aftershocks.

After defining a magnitude of completeness, 995 events with a magnitude greater than the magnitude of completeness were extracted and further analyzed. Fig. 4 shows an epicenter map of the aftershocks. The shallowest events are marked in blue, the moderately deep events with green, and the deepest with red. The results confirm that from west to east the hypocentral depth increases, thus confirming the subduction process.

### 3.3. Statistical models of aftershock occurrence

Magnitude frequency law: The occurrence of earthquakes in time and space is a complicated process, which can be examined as an aggregation of main/primary (independent) and secondary (dependent) events. For complete study of the seismicity the data for the independent and dependent events is needed.

In seismology, the distribution of earthquakes in relation with their magnitude is known as the magnitude frequency law. The earthquake frequency is given by the relation: (Equation 1)

$$\lg N_M = a - bM \tag{1}$$

where  $N_M$  is the number of events with magnitudes bigger or equal to magnitude  $M$ ,  $a$  and  $b$  are constants.

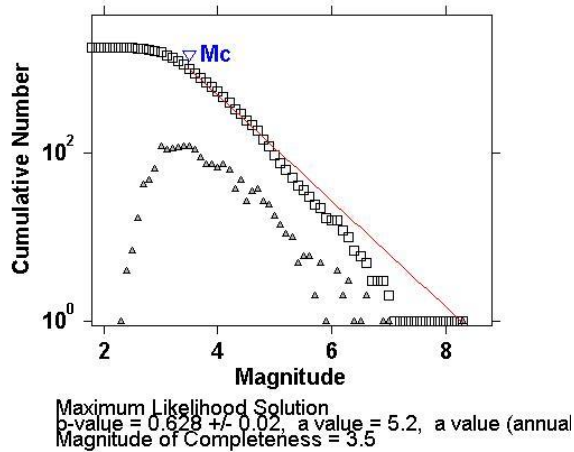


**Fig.5** Gutenberg-Richter magnitude frequency law for the examined sequence. The magnitude of completeness is  $M_w=3.5$

Due to the fact that weaker earthquakes are more frequent than stronger ones, the characterization of the seismicity of earthquake frequency is provided for the first time (Equation 1) by Gutenberg and Richter (1944). In terms of practical significance this law allows to predict the recurrence period of earthquakes with a given magnitude for a long period of time.

Aftershocks evolution in time: The first step in the statistical analysis is to examine if the earthquakes are distributed randomly in time. Due to the lack of a perfectly developed physical theory to stand in the foundation of the seismic process, usually as a starter hypothesis an independence between the seismic events is accepted.

The Japanese scientist Omori (1894) introduces in the first formula for aftershock frequency. It is defined by the equation (2) where  $t$  measures the time from the main event and  $K$  and  $c$  are constants.

$$n_a(t) = \frac{K}{t + c} \quad (2)$$

Another Japanese scientist, Utsu (1961), introduces the Modified Omori Formula (MOF) according to which the aftershock frequency at a given moment  $t$  after the main shock is given

by the equation (3) where  $t$  again measures the time from the main event,  $K$  is a parameter,  $c$  is a constant value and  $p$  is a coefficient of attenuation and may contain different values for separate stages of the aftershock sequence evolution in time.

$$n_a(t) = \frac{K}{(t + c)^p} \quad (3)$$

An issue with this model is the lack of ability for aftershocks to trigger their own series. Also, the strength of the earthquakes is not analyzed, thus the intensity of all of the secondary events cannot be linked with the magnitude of the main event.

This leads Ogata to the idea of self-similarity within the process of relaxation after a strong earthquake as all following aftershocks with magnitudes bigger or equal to the magnitude of completeness  $M_o$  value can trigger their own secondary events. In 1988 Ogata introduces a further advanced model of MOF called ETAS – Epidemic Type Aftershock Series (Ogata, 1988). To figure out the intensity of the process at a moment  $t$ , all events with a magnitude  $M \geq M_o$  are taken into account for a period of time from zero (main shock occurrence) to  $t$ .

$$\lambda(t|H_t) = \mu + \sum_{t_i < t} \frac{K_0 e^{\alpha(M_i - M_o)}}{(t - t_i + c)^p} \quad (4)$$

The conditional intensity function of such a process is given by the equation (4) in which all aftershocks are summarized. Here the  $\alpha$  parameter measures magnitude productivity in aftershocks generation.

There is a model that describes the aftershock process better, which compels both the MOF and ETAS models, called RETAS (Restricted epidemic type aftershock sequence). We shall focus on the latter model and apply it in our further analysis.

RETAS stochastic model: The model RETAS, mentioned earlier, is a model according to which secondary events can trigger only those

events, which have greater or equal to the threshold magnitude  $M_{tr}$ , also known as triggering magnitude. The idea of the model originates from the so called Bath law (1973), according to which a specific magnitude difference exists between the main earthquake and the strongest aftershock. Due to a similarity between the ETAS model, but with a restriction in terms of the triggering magnitude, this model is called RETAS – Restricted epidemic type aftershock sequence model, developed by Gospodinov and Rotondi (2006).

$$\lambda(t|H_t) = \mu + \sum_{\substack{t_i < t \\ M_i \geq M_{tr}}} \frac{K_0 e^{\alpha(M_i - M_0)}}{(t - t_i + c)^p} \quad (5)$$

The conditional density function of the RETAS model is presented by Equation (5), where the summation is performed only for aftershocks with magnitudes stronger or equal to  $M_{th}$ . The parameters in the model are similar to those in the ETAS model. To summarize,

RETAS is a model according to which secondary aftershocks can trigger only those events which have a magnitude greater or equal to the triggering magnitude  $M_{tr}$ , as the magnitude of completeness  $M_0$  is lower or equal to the triggering magnitude  $M_{tr}$  which is lower or equal to the main earthquake magnitude  $M_1$ . One of the biggest advantages of the RETAS model is that it compels both the two boundary models MOF and ETAS.

### 3.4 Stochastic modelling of the 2015 Illapel aftershock sequence

During the current research, the best variant of the RETAS model is picked according to the Akaike Information Criterion (Akaike, 1974), given by Equation (6)

$$AIC = (-2 \max \log L(Q;0,T) + 2k) \quad (6)$$

where L is the likelihood function of the model, T is the time after aftershock sequence duration, Q stands for model parameters and k is the number of model parameters.

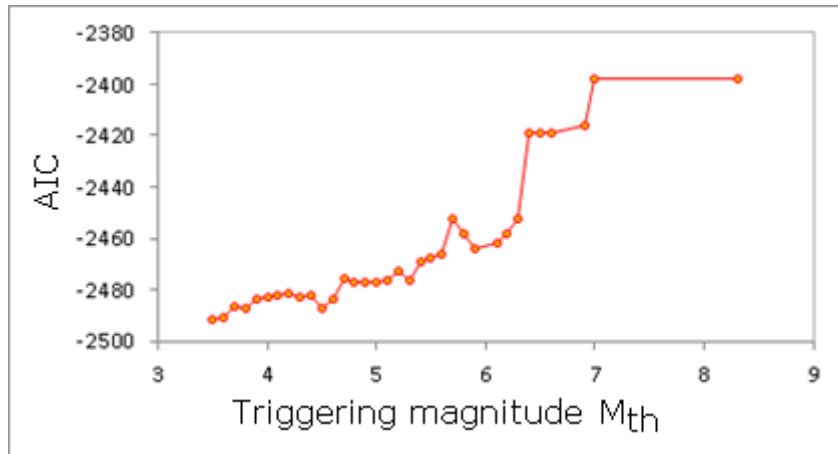


**Fig.6** Dependence of the AIC criterion on the triggering magnitude AIC. The smallest value of the criterion is for  $M_{th}=M_0$ , which means that the best fit model for our data is ETAS (see model parameter values in Table 1)

**Table 1.** Values of the of RETAS model parameters (Equation 5) of the identified best fit model for our data

$M_{th}$	$AIC$	$K$	$\alpha$	$c$	$p$
3.5	-2491.19	0.037215	1.240185	0.072663	1.056646

The smallest value of the Akaike criterion identifies the best fit variant of the RETAS

model for our data. As can be seen on Fig.6, the smallest value of the criterion is for  $M_{th}=M_0$ ,

which means that the best fit model for our data is ETAS. The aftershocks in the sequence are not clustered only to some of the strongest aftershocks, but to weaker events, too. The model parameters values of the identified model are presented in Table 1. The curve, shown on Fig.6, reveals a peculiarity, consisting in the fact that there is a decrease of the AIC value for triggering magnitudes of  $M_{th} \geq 5.8$ . This result exposes the fact that these aftershocks cause increased clustering in time after their occurrence.

In seismology, in terms of visualization, it's more convenient to show the cumulative

number of events in time. Fig. 7 shows the cumulative number of aftershocks after the main event of September 16th 2015 for a period of 8 months after. The dense blue line shows the expected theoretical number events according to the best RETAS version. The dashed blue lines stand for the error and the red dots show the real number of events. The yellow lines show the event magnitude over the elapsed time of 8 months. It's noticeable that the model describes the data well and both the graphics within the error bounds. Also, it is noticeable that some stronger aftershocks cause their own weaker series.

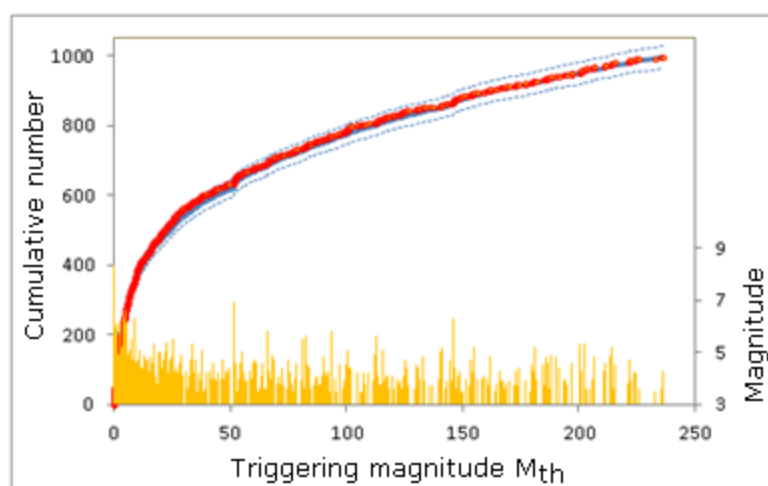


**Fig.7** Cumulative number of events with magnitude  $M_w \geq 3.5$  for the period from the first occurrence of the major earthquake to 236 days thereafter (8 months). The solid blue line represents the expected number according to the best theoretical model (ETAS). Dashed blue lines stand for the error bounds and red circles reveal the real cumulative number of aftershocks in time

## 5. CONCLUSIONS

In this study we analysed some statistical features of the aftershock sequence, subsequent to the strong earthquakes occurred in Chile on the 16th of September, 2015 with a magnitude of  $M_w=8.3$ . Except that the earthquake has a large magnitude, it also caused a tsunami wave, which motivates its detailed study. The main quake had a duration of 3 minutes and was followed by several aftershocks within the next 30 minutes, some with a magnitude greater than  $M_w > 6$ .

We first compiled aftershock catalog data, lasting 8 months after the main shock. The initial statistical analysis of the catalog,

completed with the ZMAP6.5 software, showed a relatively low b-value. This can be interpreted as an indication that there was a high number of weaker aftershocks in the series. The magnitude of completeness  $M_0=3.5$  has been estimated, only events with a magnitude less than this value were excluded.

We focused our attention on the temporal evolution of the aftershock sequence. The RETAS model was used in terms of finding a relevant time model, describing the drop in aftershock activity during the period. The estimated best-fit model turned to be ETAS, which means that the triggering magnitude was equal to magnitude of completeness.. The model

confirms such a pattern of aftershock clustering, in which aftershocks group up in time, not only along strong events, but can also form clusters after weaker shocks.

### ACKNOWLEDGEMENTS

This research was supported by the University of Plovdiv "Paisii Hilendarski", under scientific project FP17-FF-010.

### REFERENCES

Akaike, H., 1974, A new look at the statistical model identification. *IEEE Trans. Automat. Contr.* AC – 19, 716–723  
Bath, M., 1973, *Introduction to Seismology*. Birkhauser, Basel 1973  
Gospodinov, D., R. Rotondi, 2006, *Statistical Analysis of Triggered Seismicity in the Kresna*

Region of SW Bulgaria (1904) and the Umbria-Marche Region of Central Italy (1997). *Pure Appl. Geophys.* 163, 1597–1615  
Gospodinov, D., Papadimitriou, E., Karakostas, V. & Rangelov, B., 2007. Analysis of relaxation temporal patterns in Greece through the RETAS model approach, *Phys. Earth planet. Int.*, 165(3–4), 158–175.  
Gutenberg, B. & Richter, C.F., 1944. Frequency of earthquakes in California, *Bull. seism. Soc. Am.*, **34**, 185–188.  
Ogata, Y., 1988. Statistical models for earthquake occurrences and residual analysis for point processes. *J. Am. Stat. Assoc.* 83, 9–27  
Omori, F., 1894. On the aftershocks of earthquakes. *J. Colloid Sci. Imp. Univ. Tokyo* 7, 111–200  
Utsu, T., 1961. A statistical study on the occurrence of aftershocks, *Geophys. Mag.*, 30, 521–605.  
Wiemer S., 2001. A Software Package to Analyze Seismicity: ZMAP. *Seism. Res. Lett.* 72, 373–382